colloids and interfaces

MDPI

Article

Adsorption and Desorption of Bile Salts at Air–Water and Oil–Water Interfaces

Teresa del Castillo-Santaella [1] and Julia Maldonado-Valderrama [2,3,*]

[1] Department of Physical Chemistry, Faculty of Pharmacy, University of Granada, Campus de Cartuja sn, 18071 Granada, Spain
[2] Department of Applied Physics, Faculty of Sciences, University of Granada, Campus de Fuentenueva sn, 18071 Granada, Spain
[3] Excellence Research Unit "Modeling Nature" (MNat), University of Granada, 18071 Granada, Spain
* Correspondence: julia@ugr.es

Abstract: Bile Salts (BS) adsorb onto emulsified oil droplets to promote lipolysis and then desorb, solubilizing lipolytic products, a process which plays a crucial role in lipid digestion. Hence, investigating the mechanism of adsorption and desorption of BS onto the oil–water interface is of major importance to understand and control BS functionality. This can have implications in the rational design of products with tailored digestibility. This study shows the adsorption and desorption curves of BS at air–water and oil–water interfaces obtained by pendant drop tensiometry. Three BS have been chosen with different conjugation and hydroxyl groups: Sodium Taurocholate (NaTC), Glycodeoxycholate (NaGDC) and Sodium Glycochenodeoxycholate (NaGCDC). Experimental results show important differences between the type of BS and the nature of the interface (air/oil–water). At the air–water interface, Glycine conjugates (NaGDC and NaGCDC) are more surface active than Taurine (NaTC), and they also display lower surface tension of saturated films. The position of hydroxyl groups in Glycine conjugates, possibly favors a more vertical orientation of BS at the surface and an improved lateral packing. These differences diminish at the oil–water interface owing to hydrophobic interactions of BS with the oil, preventing intermolecular associations. Desorption studies reveal the presence of irreversibly adsorbed layers at the oil–water interface in all cases, while at the air–water interface, the reversibility of adsorption depends strongly on the type of BS. Finally, dilatational rheology shows that the dilatational response of BS is again influenced by hydrophobic interactions of BS with the oil; thus, adsorbed films of different BS at the oil–water interface are very similar, while larger differences arise between BS adsorbed at the air–water interface. Results presented here highlight new features of the characteristics of adsorption layers of BS on the oil–water interface, which are more relevant to lipid digestion than characteristics of BS adsorbed at air–water interfaces.

Keywords: bile salts; adsorption; desorption; air–water interface; oil–water interface; interfacial tension; surface tension; dilatational elasticity; lipid digestion; lipolysis

Citation: del Castillo-Santaella, T.; Maldonado-Valderrama, J. Adsorption and Desorption of Bile Salts at Air–Water and Oil–Water Interfaces. *Colloids Interfaces* **2023**, *7*, 31. https://doi.org/10.3390/colloids7020031

Academic Editor: Georgi G. Gochev

Received: 23 February 2023
Revised: 30 March 2023
Accepted: 3 April 2023
Published: 11 April 2023

1. Introduction

Lipolysis is an interfacial process that occurs in the gastrointestinal tract during the digestion of emulsified lipids. In this process, bile salts (BS), lipase and co-lipase adsorb onto the oil–water interface of emulsion droplets to hydrolyze triglycerides (lipids) into free fatty acids and monoglycerides, which also compete for the oil–water interface. Then, BS solubilize free fatty acids in mixed micelles that are absorbed through intestinal microvillosities. Accordingly, BS collaborate in two essential physiological functions involving lipids: lipid digestion and absorption. First, BS promote lipase and co-lipase binding to the oil–water interface, promoting lipolysis. Second, BS desorb from the oil–water interface, solubilizing free fatty acids into the intestinal mucosa for their posterior absorption [1,2]. For these two functions of BS, understanding the adsorption and desorption behavior of BS from oil–water interfaces represents a critical step.

BS are amphiphilic molecules with a planar polarity, unlike linear amphiphilic compounds (head-polar and tail-apolar). The amphiphilic nature of BS causes the spontaneous formation of micelles, which solubilize and transport lipolysis products (fatty acid and monoglycerides) into the mucosa of the small intestine for their absorption. Because of the planar structure of BS, they form peculiar micelles. Namely, they have low aggregation numbers of 3 to 11 BS units and relatively low CMC values (2 to 20 mM) [3]. Furthermore, simulation studies showed that BS in micelles can change their aspect ratio from oblate to spherical and prolate [4]. This special conformation of BS micelles is essential to ensure the transport and release of products from lipolysis, nutrients and drugs. The planar structure of BS is also responsible for a peculiar surface activity of BS, which has been reviewed in some recent studies [2,3,5].

BS present a rigid structure consisting of a convex-hydrophobic side formed by the rigid steroid ring system and a concave-hydrophilic side with one, two or three hydroxyls and an amino group conjugated with Glycine, Taurine or other amino acids (Figure 1). The classification of BS differs in the number and position of the hydroxyl groups, which can be 3, 7 or 12, and the conjugated amino acids [6]. BS come from bile acids derived from the oxidation of cholesterol in the liver. BS are conjugated with either 75% Glycine (hydrophobic) or 25% Taurine (hydrophilic). Cholates with three hydroxyl groups (at positions 3, 7 and 12) and Chenodeoxycholates with two hydroxyl groups (at positions 3 and 7), comprise 41% and 43%, respectively, while Deoxycholates with two hydroxyl groups (at positions 3 and 12) represent 12% and other bile acids comprise 5% of total BS [6]. These chemical differences between BS result in slight differences in their surface activity, which have been explored in the literature to some extent but are not yet fully understood [2,3,5,7,8]. A rather complete work was published by Parker et al. reporting differences in the adsorption/desorption behavior onto solid hydrophobic surfaces by using dual polarization interferometry [6]. In particular, Deoxycholates and Chenodeoxycholates adsorbed more rapidly than Cholates and desorbed to a greater extent following buffer rinsing. Conjugating groups (Taurine, Glycine) did not have an impact on the surface behavior. Results from our laboratory also highlighted differences in the adsorption/desorption of BS at the air–water interface with pendant drop tensiometry [9]. Following subphase exchange with buffer, Deoxycholate desorbed from the air–water interface to a greater extent than Cholate. However, the surface activity of Chenodeoxycholate was not reported therein. The importance of the chemical composition of BS has also been addressed by Łozińska and Jungnickel, who showed recently that NaTC increases the lipolysis rate with respect to its unconjugated counterpart, NaDC [10].

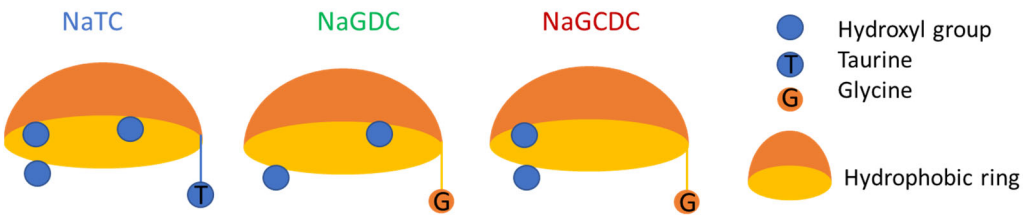

Figure 1. Schematic representation of Bile Salts used in this work. NaTC (Sodium Taurocholate), NaGDC (Sodium Glycodeoxycholate) and NaGCDC (Sodium Glycochenodeoxycholate).

In view of these results, it appeared interesting to complete the surface characterization of BS with data from Chenodeoxycholates and to compare them with the adsorption/desorption of BS from oil–water interfaces as a more physiologically relevant model for emulsified systems [10]. The behavior of surfactants at the air–water interface is generally used as a model for the oil–water interface since experiments at the air–water interface are easier to perform. However, the presence of an oil–water interface can promote/hinder intermolecular associations and conformational/orientational changes in the adsorbed layer, as demonstrated for other biosurfactants [7,11–13]. To our knowledge, a systematic comparison between BS films adsorbed at air–water and oil–water interfaces has not been

reported so far. Herein, adsorption, desorption and dilatational properties are reported for BS at air–water and oil–water interfaces. Three BS, with different hydroxyl groups (Cholate, Deoxycholate and Chenodeoxycholate) and different conjugation groups (Taurine and Glycine) are compared (Figure 1). Accordingly, results shown here comprise a thorough surface/interfacial characterization of BS which highlights the impact of both the interface and the nature of BS on their interfacial activity. The study of the behavior of BS at the oil–water interfaces is essential to understand the mechanisms of lipid digestion and to rationally design products with tailored digestion profiles, such as anti-obesity or targeted delivery systems.

2. Materials and Methods

2.1. Materials

Sodium Taurocholate (NaTC, cat n. 86339), Glycodeoxycholate (NaGDC, cat n. G9910) and Sodium Glycochenodeoxycholate (NaGCDC, cat n. G0759) were purchased from Sigma-Aldrich® (Darmstadt, Germany) and used as received. The buffer used in all solutions was 2 mM Bis-Tris (Sigma-Aldrich®, cat n. 14879, Darmstadt, Germany), 150 mM Sodium Chloride (Scharlau, cat n. SO02251000, Barcelona, Spain) and 10 mM Calcium Chloride (Sigma-Aldrich®, cat n. C4901, Darmstadt, Germany) adjusted to pH 7.0. This buffer mimics the physiological conditions of the duodenum [14]. Figure 1 shows a schematic representation of BS structure, highlighting the conjugation and position of hydroxyl groups in the molecule.

Ultrapure water (0.054 µS) from a Milli-Q water purification system was used for buffer preparation. All glassware was cleaned with 10% Micro-90 cleaning solution, rinsed with tap water, isopropanol, deionized water, and ultrapure water in this sequence.

Highly refined olive oil (Sigma-Aldrich®, cat no. 01514, Darmstadt, Germany) was purified with Florisil® resins (Fluka, 60–10 mesh, cat no. 46385, Sigma-Aldrich®, Darmstadt, Germany) before use by following the procedure used in previous studies [7,15,16]. Namely, a mixture of oil and Florisil® (Sigma-Aldrich®, cat no. 46385, Darmstadt, Germany) in a 2:1 proportion w/w was shaken mildly for 2 h and then centrifuged at 14,300 rpm for 30 min in a centrifuge from Kronton instruments (Centrikon T-124). The olive oil/resins mixture was filtered with Millex® filters (0.1 µm PDVF, Sigma-Aldrich®, cat no. F7523, Darmstadt, Germany) and stored under nitrogen in dark bottles until use.

All the experiments were recorded at 37 °C and monitored by external temperature control. The surface tension of the water/buffer droplet in air and the interfacial tension of the water/buffer droplet immersed in oil were measured before every experiment to confirm the absence of surface-active molecules and were 70.7 ± 0.5 mN m^{-1} and 27.5 ± 0.5 mN m^{-1}, respectively, at 37 °C.

2.2. Pendant Drop Surface Film Balance with Subphase Exchange: OCTOPUS

All the experiments were made in the OCTOPUS, a pendant-drop surface balance equipped with a subphase multiexchange device which was fully designed and assembled at the University of Granada (Figure 2) [9,15]. The pendant drop was formed inside a glass cuvette (Hellma®, Jena, Germany) located inside a cell connected to a thermostat (37 °C). For measurements at the oil–water interfaces, the cuvette was filled with the purified oil phase. The drop was formed at the tip of a Teflon capillary, which was composed of an arrangement of two coaxial capillaries [17] that were independently connected to each channel of a double microinjector (PSD3, Hamilton®, Giarmata, Romania). Each microinjector had a syringe allowing the filling or emptying to occur independently (to clean) or coordinately (to exchange the droplet subphase). The OPTOPUS had eight via valves, with each via connected by a tube to different solutions [18]. The drop was illuminated by a light source and drop images were captured by a CCD video camera (Pixelink®, Ottawa, ON, Canada) connected to an optical microscope (Edmund Optics Ltd., York, UK). The whole system is computer controlled by the software DINATEN© [18,19] which automatically extracts experimental drop profiles and fits it to the Young–Laplace

equation of capillarity by using ADSA, (Axisymmetric Drop Shape Analysis) providing as outputs the volume, the surface/interfacial tension (ST, IT), and the surface/interfacial area (A) of the pendant drop.

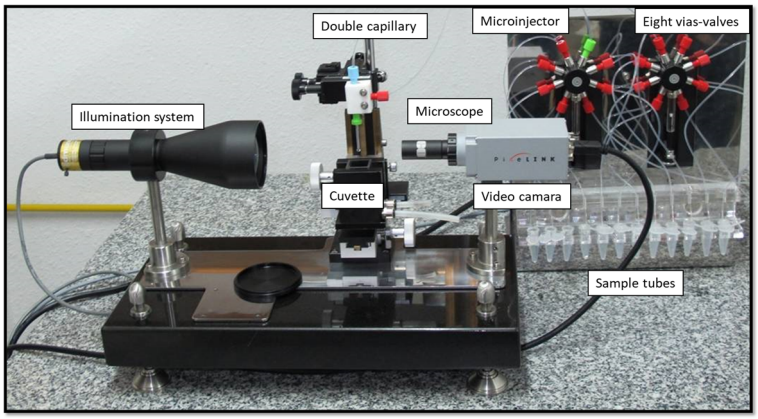

Figure 2. The OCTOPUS: Pendant Drop Tensiometer equipped with Multiexchange device (Producciones Científicas Y Técnicas, Gójar, Spain). Adapted from [18] with permission from J. Vis. Exp. 2022.

The dilatational rheology of adsorbed layers was measured by imposing periodic area deformations to the interfacial layer by controlled injection/extraction of solution into the pendant drop. DINATEN® (Producciones Científicas Y Técnicas, Gójar, Spain) records the response of surface/interfacial tension ($\Delta\gamma = \gamma(t) - \gamma^0$) to the area deformation, given by the relative area variation ($\alpha = \Delta A/A0 = (A(t) - A^0)/A^0$). The dilatational stress can be written as the sum of two terms: one purely elastic, proportional to the surface deformation (α), and one a viscous term, proportional to the rate of surface deformation ($d\alpha/dt$) [20]:

$$\Delta\gamma = \varepsilon\alpha + \eta\frac{d\alpha}{dt} \quad (1)$$

where coefficients ε and η are the interfacial elasticity and viscosity, respectively. For low amplitude periodic deformations of frequency ν, the area change can be expressed as:

$$\Delta A = Ae^{2\pi\nu t} \quad (2)$$

Introducing Equation (2) in 1 provides the dilatational complex dilatational modulus E:

$$E = \frac{\Delta\gamma}{\Delta A/A^0} = \varepsilon + i2\pi\nu\eta = E' + iE'' \quad (3)$$

Accordingly, E is a frequency-dependent complex quantity, where the real part E' accounts for the dilatational elasticity (ε) and the imaginary part E'' accounts for the dilatational viscosity (η). To avoid excessive perturbation of the interfacial layer, the applied oscillations were made at deformation values $\Delta A/A^0 < 5\%$. Images from DINATEN® were processed by the software CONTACTO®, which calculated the dilatational parameters from the dilatational stress, the deformation, and their phase shift by applying Equation (3). Further details of this procedure can be found elsewhere [20]. The frequency was fixed at 1 Hz in all measurements, which is a relatively high value to maximize the elastic response, as will be discussed later [12].

The desorption of BS was assessed by recording the surface/interfacial tension as the droplet subphase (solution) was exchanged with buffer. This was carried out using the double capillary, which allows an automatic, non-invasive interface and complete exchange of the subphase of the drop, preserving the droplet area [9]. Bulk depletion of the droplet solution promoted spontaneous desorption of soluble and/or reversibly adsorbed molecules from the interface owing to the concentration gradient, resulting in

an increase of the surface/interfacial tension. The subphase exchange continued until the subphase was fully depleted of BS and the surface/interfacial tension reached a steady value corresponding either to a bare interface or to an irreversibly adsorbed layer.

In this work, the interfacial area of the drop was fixed at 20 mm^2 during the adsorption and desorption phases, lasting 1 h each. The range of concentrations of BS varied between 10^{-6} M and 10^{-1} M in buffer simulating the physiological conditions of small intestines, and the temperature was fixed at 37 °C.

3. Results and Discussion

As already stated, BS are surface active molecules with a planar structure which impacts the surface/interfacial activity compared with linear amphiphilic molecules with a head–tail distribution (head-hydrophilic and tail-hydrophobic). The structure of BS resembles a spoon where the convex part is hydrophobic and the concave is hydrophilic, and it contains conjugation groups (Glycine or Taurine) and hydroxyl groups (two or three) [2,3]. This peculiar structure promotes rapid adsorption onto surfaces/interfaces, which facilitates lipolysis, and the formation of fluid and mobile films, which facilitate the transport of lipolytic products [2,3]. The adsorption rate and the interfacial attachment can be assessed by measuring the adsorption and desorption profiles of BS at air– or oil–water interfaces, respectively [9]. First, the adsorption isotherms of three BS (NaTC, NaGDC and NaGCDG) are compared at air/oil–water interfaces. Second, the desorption of these BS is analyzed at the two interfaces. Finally, the dilatational moduli of BS films adsorbed at air/oil–water interfaces are reported. Combined analysis provides new information on the mechanical and structural properties of BS films and how they impact functionality through adsorption/desorption.

3.1. Adsorption of BS onto Air–Water and Oil–Water Interfaces

Figure 3a shows the surface/interfacial tension attained after 1 h adsorption of different concentrations of NaTC, NaGDC and NaGCDC at air/oil–water interfaces. At the lowest concentrations, the values remain close to that of clean air/oil–water interfaces. This is due to the number of molecules adsorbed being low and non-interacting, so the surface/interface tension remains unchanged. As the number of adsorbed molecules increases at the interface, the surface/interfacial tension decreases. Above a certain critical concentration, the surface/interfacial tension becomes independent of the concentration. This critical concentration is called the Critical Micelle Concentration (CMC) of amphiphiles and is determined by the chemical potential balance between a micelle and a monomer surfactant. In micelles, amphiphilic molecules orient their hydrophilic heads outwards and the hydrophobic tails inwards. Hence, the surface of micelles is hydrophilic and does not have surface/interfacial activity. Concerning the minimum value of the surface tension (Figure 3a), this is reached at the air–water interface (around 45 mN/m), and it is relatively high compared to values reached by linear head–tail surfactants [21]. Conversely, at the oil–water interface, the interfacial tension reaches quite low values (below 10 mN/m) (Figure 3a). This fact already indicates possible differences in the lateral packing of BS at air/oil–water interfaces, owing to a hydrophobic interaction with the oil. Also, the shape of the isotherms shows slight slope discontinuities in agreement with literature reports [22].

A remarkable feature in Figure 3a is that different BS display significant differences in their adsorption isotherms at the air–water interface, while these differences seem to diminish at the oil–water interface (Figure 3a). At the air–water interface, NaGCDC appears more surface active, followed by NaGDC and NaTC (Figure 3a). Conversely, at the oil–water interface, the adsorption isotherms of NaGDC and NaGCDC overlap, while NaTC appears just slightly displaced to higher bulk concentrations, indicative of lower interfacial activity (Figure 3a). The trends are similar at air/oil interfaces; the presence of Taurine (NaTC) reduces the surface/interfacial activity compared to Glycine (NaGDC and NaGCDC). This trend also correlates with other studies reporting that the amphiphilicity

of BS is influenced by the Cholate conjugation group, with Glycine-conjugates being more hydrophobic than Tauro-conjugates [9,22].

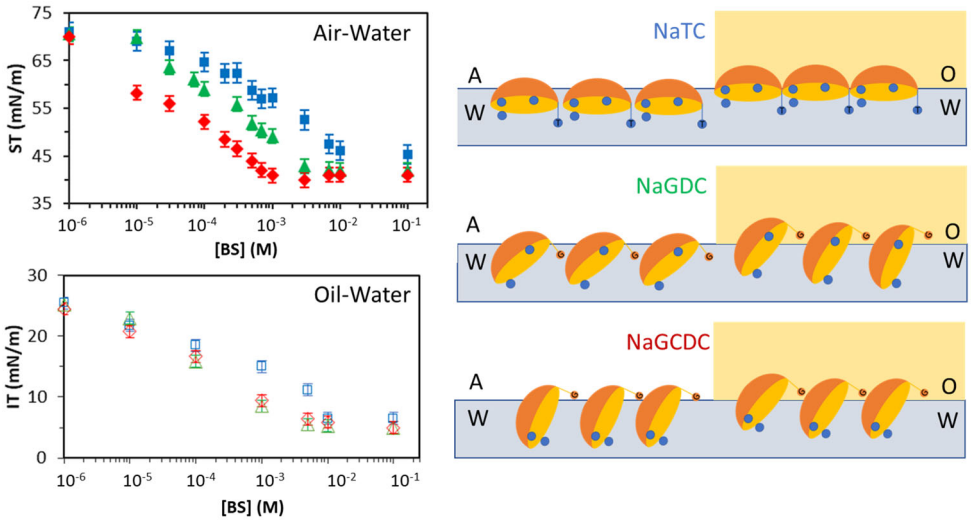

(**a**) (**b**)

Figure 3. (**a**) Surface/interfacial tension (ST/IT) versus concentration of BS ([BS]) after 1 adsorption of NaTC (blue squares), NaGDC (green triangles) and NaGCDC (red rhomboids) at air–water (solid symbols) and oil–water (open symbols) interfaces in 2 mM Bis-Tris, 150 mM NaCl, 10 mM $CaCl_2$, pH 7, T = 37 °C. Mean values with error bars representing standard deviations from three independent experiments. (**b**) Schematic diagram of the proposed orientation of NaTC, NaGDC and NaGCDC at air/oil–water interfaces.

Apart from the conjugation group, the number and position of hydroxyl groups in BS (Figure 1) also affect the adsorption isotherms recorded (Figure 3a). At the air–water interface, the surface activity of BS decreases in this order: Chenodeoxycholate > Deoxycholate > Cholate. At the oil–water interface, the interfacial activity follows this trend: Chenodeoxycholate = Deoxycholate > Cholate. This can be further appreciated by analyzing the values of the CMCs as calculated in Figure 3a. In fact, CMCs are clearly identified at the air–water interface, with the lowest CMC value obtained for Chenodeoxycholate (NaGCDC, ~1 mM), closely followed by Deoxycholate (NaGDC, ~2 mM), while the highest CMC corresponds to Cholate (NaTC, ~10 mM). These results agree qualitatively with those reported in the literature for BS [1,3]. An explanation for this is found in Cholate having three hydroxyl groups (Figure 1) and therefore being more hydrophilic. Thus, it provides a lower surface/interfacial activity and higher CMC (Figure 3a). Chenodeoxycholate and Deoxycholate both have two hydroxyl groups (Figure 1) and hence provide more similar CMCs, which are lower than Cholate's (Figure 3a). Then again, the position and proximity of the two hydroxyl groups (3 and 7) at the bottom of the rigid steroid ring might explain the slight but significant difference in CMCs spotted at the air–water interface for NaGCDC and NaGDC (Figure 3a). Figure 3b shows a schematic diagram of a possible packing and orientation of BS at the air/oil–water interface. This representation (Figure 3b) is hypothesized in view of the surface/interfacial activity and CMCs inferred from Figure 3a. However, a more detailed analysis of the displacements and orientations of BS at interfaces would be required to ensure the validity of the representation depicted. It is hypothesized that NaTC should lie rather planar at the surface orienting hydrophilic Taurine and three hydroxyls towards the water. Conversely, NaGDC and NaGCDC should lie more vertically, orienting the more hydrophobic Glycine towards the air phase. This verticality could be favored by the close positions of hydroxyl groups in NaGCDC, which tend to remain in the water (Figure 3b). This proposed improved packing would also explain the lowest surface tension values obtained for NaGCDC followed by NaGDC and NaTC.

The CMC values are less distinguishable at the oil–water interface as the curves appear smoother (Figure 3a). However, the obtained results correlate with findings at the air–water interface, producing a similar CMC for Cholate (NaTC, ~10 mM); this is again higher than Chenodeoxycholate and Deoxycholate, which now show a similar CMC (~3 mM). This value is slightly higher than that obtained at the air–water interface and this again correlates with an improved packing achieved at the oil–water interface. This agrees with orientational differences of BS upon adsorption onto air/oil–water interfaces as proposed in Figure 3b. Other authors report different surface/interfacial activity of surfactants. Wojciechowski et al. showed a higher interfacial activity of the Quillaja bark saponin at an olive oil–water interface compared to an air–water interface [23]. Similar results have been published recently, where sunflower proteins adsorbed differently at air/oil–water interfaces [24]. A recent work compared the adsorption of surfactants onto different fluid interfaces and claimed that linear surfactants compete with polar oil molecules at the interface, resulting in a lower interfacial packing and larger interfacial area at oil–water interfaces [21]. However, findings from Figure 3a suggest a different trend when comparing BS at air/oil–water interfaces, which are depicted in Figure 3b. At the air–water interface, the lack of hydrophobic interactions with the air phase might result in lower surface packing and larger molecular areas while the BS molecules protrude into the oil phase, hence compensating for the orientational differences at the air–water interface and explaining the more similar behavior found for BS adsorption onto an oil–water interface. Furthermore, an improved packing at the oil–water interface would also explain the low values of interfacial tension reached and the higher CMCs obtained for BS at oil–water interfaces (Figure 3).

3.2. Desorption of BS from Air–Water and Oil–Water Interfaces

Figure 4 shows the dynamic adsorption–desorption profiles recorded with the OCTOPUS for NaTC, NaGCD and NaGCDC at a single concentration of 0.1 mM at the air–water (Figure 4a) and at the oil–water (Figure 4b) interfaces.

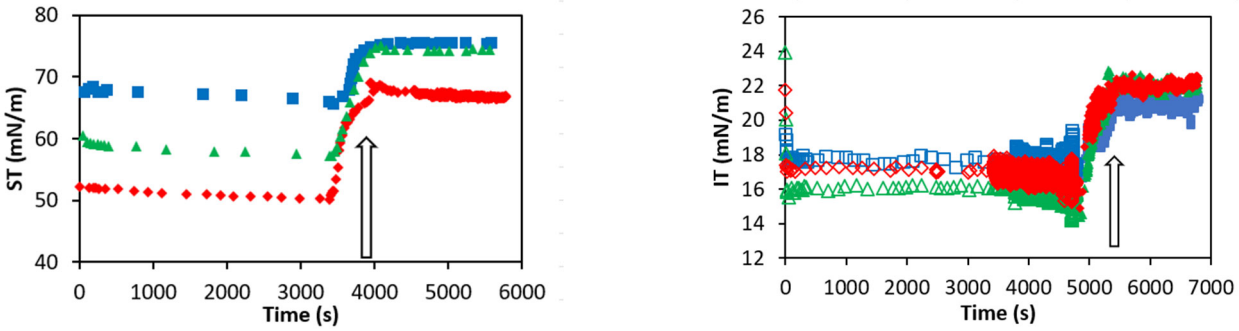

Figure 4. Adsorption–desorption profile of NaTC (blue squares), NaGCD (green triangles) and NaGCDC (red rhomboids) at the (**a**) surface tension (ST) at the air–water interface (solid symbols); and (**b**) interfacial tension (IT) at the oil–water interface (open symbols). BS concentration is 0.1 mM, in 2 mM Tris, 150 mM NaCl, 10 mM $CaCl_2$ at pH 7, T = 37 °C. The curves represented are the mean of three independent experiments with a standard deviation $\leq$ 2 mN/m (not plotted).

Figure 4 again highlights significant differences between the adsorption/desorption profiles of different BS at the air/water interface which practically vanish at the oil–water interface. At the air–water interface (Figure 4a), the adsorption process is very rapid, and a practically constant value of surface tension is reached immediately after drop formation. At the oil–water interface (Figure 4b), the adsorption process is also very rapid, but some dynamic data are recorded within the first seconds. Nonetheless, the adsorption kinetics of BS is hardly measurable by pendant drop tensiometry, and hence only steady-state values of surface/interfacial tension will be discussed herein. This result differs from proteins which

show a slower dynamic of adsorption at the air/oil–water interface [15,16,25]. The different adsorption behaviour of NaTC, NaGDC and NaGCDC at the air–water interface has already been discussed in the previous section. Figure 4 shows that NaTC attained a final surface tension of 65 ± 2 mN m^{-1}, NaGDC reached 55 ± 2 mN m^{-1} and NaGCDC reached 50 ± 2 mN m^{-1} (air–water). This trend is consistent with Taurine being more hydrophilic and NaTC having three hydroxyl groups, as discussed in detail above. Conversely, the more hydrophobic Glycine is possibly responsible for the lower surface tension reached by NaGDC and NaGCDC (Figure 3a). Finally, the different positions of hydroxyl groups in Deoxycholate and Chenodeoxycholate could explain differences in the surface tension attained for NaGDC and NaGCDC. As discussed above, we hypothesize that the closer position of hydroxyl groups in NaGCDC might result in a more vertical orientation of the molecule allowing for better packing and explaining the lower surface tensions (Figure 3). The desorption profile reported for BS at the air–water was analyzed by the evolution of the surface tension as the bulk subphase of the drop is exchanged with buffer, and it is indicated with an arrow in Figure 4. At the air–water interface (Figure 4a), the surface tension increases after subphase exchange. In particular, for NaTC and NaGCD, the surface tension practically recovers the value of the clean air–water interface and is hence indicative of complete desorption of the adsorbed layer. In contrast, for NaGCDC, the surface tension increases after subphase exchange but does not recover the value corresponding to the clean interface. Accordingly, some irreversibly adsorbed NaGCDC remains at the surface after bulk depletion, at least at this bulk concentration (Figure 4a).

Figure 4b shows the adsorption and desorption profiles of the three BS recorded at the oil–water interface. The interfacial tensions attained after 1 h of adsorption were between 17 and 15 mN/m, and the curves practically overlap. This is consistent with findings from Figure 3a and the proposed orientation of BS monolayers depicted in Figure 3b. Concerning the desorption profile, in all three cases, the interfacial tension increased after the subphase exchange but did not recover the value of the clean oil–water interface. Accordingly, some irreversibly adsorbed BS remain at the oil–water interface for NaTC, NaGDC and NaGCDC (Figure 4). A reason for this could again originate from the improved hydrophobic interaction with the oil as proposed in Figure 3b.

The dynamic curves shown in Figure 4 reveal important differences in the adsorption/desorption profiles of BS at air/oil–water interfaces. Therefore, the adsorption/desorption profiles of BS were measured for the rest of the concentrations plotted in the adsorption isotherms (Figure 3), and the results are summarized in Figure 5, namely, the steady state surface/interfacial tension attained after adsorption/desorption of BS at the air–water (Figure 5a) and at the oil–water (Figure 5b) interfaces during the 1 h period. Again, it is worth mentioning the differences between the desorption of BS from the air–water interface (Figure 5a), which practically vanish at the oil–water interface (Figure 5b).

At the air–water interface (Figure 5a), the surface tension obtained after desorption revealed the presence of different irreversibly adsorbed layers. In all cases, the amount of irreversibly adsorbed material increased as the bulk concentration increased, shown by the lower surface tensions obtained after desorption for the highest concentrations. This has been already reported in the literature and is related to surface aggregation/complexation at high concentrations of BS [8,9]. However, the three BS analyzed also display subtle differences in the desorption profiles at the air–water interface (Figure 5a). NaGDC fully desorbs from the surface as the surface tension recovers the value of the pure air–water interface within all the concentration ranges. NaTC reveals the presence of irreversibly adsorbed film only at the highest bulk concentration (10 mM). Finally, NaGCDC shows an irreversibly adsorbed layer at a concentration above 1 mM. Differently, at the oil–water interface (Figure 5b), in all cases, the interfacial tension obtained after desorption revealed the presence of some irreversibly adsorbed material, especially for Glycine-conjugates, as measured by the lower interfacial tension of 10 mM curves obtained for NaGDC and NaGCDC after desorption. This trend agrees with the more hydrophobic nature of Glycine compared to Taurine and again suggests the existence of hydrophobic interactions with

oil promoting irreversible adsorption to some extent, maybe via surface complexation, as suggested by [8].

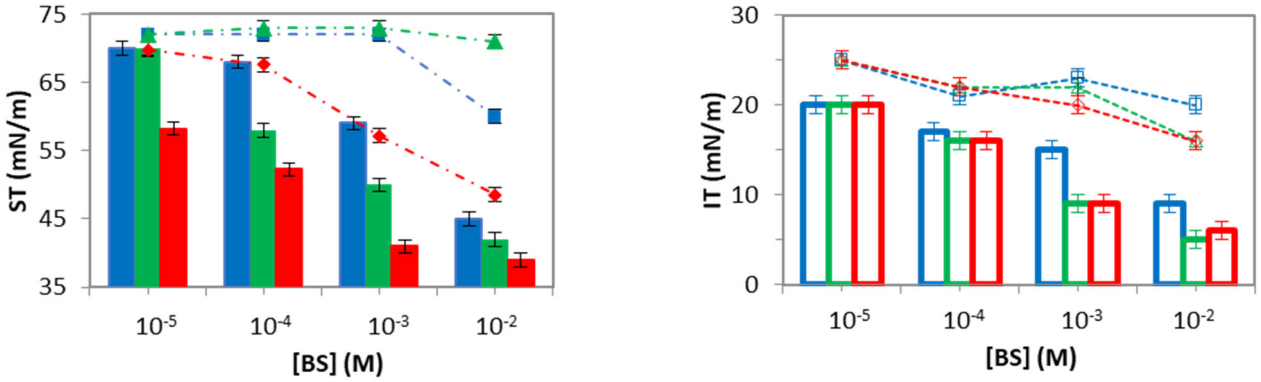

(**a**) (**b**)

Figure 5. (**a**) Surface tension (ST), solid bars and symbols; and (**b**) interfacial tension (IT), empty bars and symbols, attained after 1 h of adsorption (bars) followed by 1 h of desorption (symbols), plotted versus concentration of BS ([BS]) for NaTC (blue, squares), NaGDC (green, triangles) and NaGCDC (red, rhomboids) in 2 mM Bis-Tris, 150 mM NaCl, 10 mM $CaCl_2$, pH 7, T = 37 °C. Mean values are plotted with standard deviations from three independent experiments included as error bars.

The adsorption/desorption profiles of BS from a solid surface were studied by dual polarization interferometry by Parker et al. [6]. Remarkably, the results obtained therein reproduce qualitatively the observed trend here for BS desorption at the air–water interface (Figure 4a andFigure 5a). Specifically, Parker et al. showed that Cholates adsorbed irreversibly to solid surfaces while Deoxycholates desorbed completely after washing with buffer, regardless of the conjugation group [6]. Those measurements were performed under similar conditions (3 mM BS and 2 mM Bis-Tris, pH 7.0, 150 mM NaCl and 0–10 mM $CaCl_2$). According to Parker et al., Chenodeoxycholate also adsorbed irreversibly onto solid surfaces, but its behavior was more dependent on the conjugation group [6]. Moreover, atomic force microscopy images showed that NaGDC adsorbed as disrupted structures which could be desorbed, in contrast to NaTC, which adsorbed as a continuous film with a granular texture [6]. Accordingly, adsorption/desorption of BS at a solid surface correlates largely with that seen at the air–water interface (Figure 5a) but differs significantly from that obtained at the oil–water interface (Figure 5b). Indeed, the hydrophobic interaction of BS with oil might induce orientational differences with respect to a non-interacting air and solid interface, as recently reported for linear surfactants [21]. A hypothesis for the different desorption profiles encountered for BS at the air–water interface could be found again in the positions of hydroxyl groups in the molecule. These are in closer positions in NaGCDC (positions 3 and 7), while they appear at the extremes of the concave side for NaTC (3, 7, 12) and NaGDC (3 and 12) (Figure 1). Having the hydroxyl groups in closer positions and located on the same side might favor the surface complexation of NaGCDC at the air–water interface, which could be responsible for irreversible adsorption. Given that, at the oil–water interface, the hydrophobic interaction possibly determines the desorption profile. The conjugation group plays a major role in desorption, as also happens in the adsorption profile (Figure 3). Figure 5b shows that Glycine conjugates display a lower interfacial tension after desorption, meaning that Glycine conjugates adsorbed more irreversibly than Taurine conjugates at the oil–water interface. The hydrophilic interaction of hydroxyl groups seems irrelevant at the oil–water interface, as the desorption behavior of NaGDC and NaGCDC is completely similar (Figure 5b).

According to these results, the different compositions of the interface can affect the level of adsorption and desorption of surface-active molecules and how they are oriented and anchored at the interface. Experiments at the air/solid interface reveal important

differences with respect to the oil–water interface. A reason for this can be the lack of hydrophobic interactions with the air/solid phase, which are present at oil–water interfaces, hence altering the adsorption and the desorption. Moreover, the conjugation of groups determines the anchoring at the oil–water interface, while the number/location of hydroxyl groups seems to impact the desorption from the air–water interface. Hence, the hydrophobic interaction with conjugates at the oil–water interface could determine interfacial complexation and, hence, desorption profiles of BS. The final section evaluates the dilatational viscoelasticity of adsorbed films to shed light on this speculation and to look into the surface/interfacial conformation of different BS upon adsorption to air/oil–water interfaces.

3.3. Dilatational Elasticity of BS Adsorbed at Air–Water and Oil–Water Interfaces

The mechanical response of an interface to a small harmonic area deformation was measured at a fixed frequency of 1 Hz by increasing/decreasing the drop volume. This provides the dilatational viscoelasticity of the surface/interfacial layer, which contains information on the organization and interactions of molecules adsorbed at air/oil–water interfaces, highlighting composition, orientations, and intermolecular forces and associations [9,15,16,26]. The behavior of the dilatational modulus of interfacial layers depends on the bulk concentration and on the oscillation frequency [27]. For soluble surfactants, upon monolayer compression/expansion, some surfactant molecules dissolve into the bulk/adsorb back onto the surface to restore the equilibrium surface concentration. At the low-frequency limit, the monolayer always has time to adapt to deformation and recover equilibrium, and the dilatational stress is zero (Equation (1)). At the high-frequency limit, the monolayer has no time to adapt to deformation and the interfacial stress is mostly elastic, as the monolayer behaves as if it were insoluble. At an intermediate frequency range, there is an elastic and viscous contribution to the dilatational stress. BS are highly surface-active molecules, and the applied oscillation frequency was the highest compatible with the instrument, i.e., 1 Hz, so as to minimize the viscous response of the interfacial layer. In addition, this high frequency/insoluble monolayer regime provides an elastic response only for a monolayer, i.e., at low bulk concentrations, whereas at higher bulk concentrations, the interfacial layer adapts to the deformation, instantaneously reducing the dilatational stress [27]. Figures 6 and 7 show the storage and loss modulus (Equation (3)) of BS-adsorbed layers at the air–water and oil–water interfaces, respectively. In both cases, $E'' << E'$ is indicative of the elastic nature of the interfaces formed. The dependence of E' with the bulk concentration matches that predicted for soluble surfactants. Namely, E' increases with bulk concentration to a maximum, followed by a gradual decrease, providing a practically null dilatational response at the highest bulk concentrations.

At the air–water interface (Figure 6), the location of the maximum in the concentration range follows the same trend as the CMC: NaGCDC < NaGDC < NaTC. In addition, Glycine-conjugates (NaGDC and NaGCDC) display a similar value of maximum elasticity (~40 mN/m) that was significantly higher than that of Taurine conjugate (NaTC, ~20 mN/m), which also shows a second maximum of (~15 mN/m) located at higher bulk concentrations. A maximum dilatational modulus corresponds to the formation of a cohesive surface layer in which the molecules spread at the surface in a single conformation. The height of the maximum relates to the molecular interconnections at the surface/interfacial layer. The stronger dilatational response of Glycine-conjugates at the air–water interface agrees with the higher surface activity and the improved surface packing discussed and schematized in Figure 3. Similarly, a lower dilatational elasticity suggests the formation of a more fluid surface layer, with fewer lateral interactions [9].

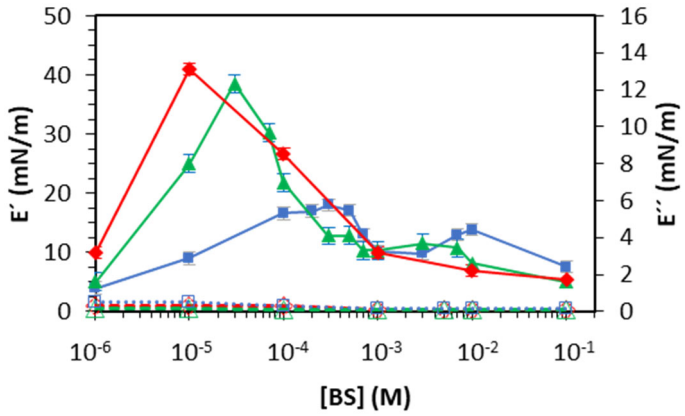

Figure 6. Storage moduli (E′, solid symbols) and loss moduli (E″, open symbols) of NaTC (blue squares), NaGDC (green triangles) and NaGCDC (red rhomboids) at different concentrations of BS ([BS]) at the air–water interface. Dilatational parameters were measured after 1 h of adsorption at a frequency of 1 Hz in 2 mM Bis-Tris, 150 mM NaCl, 10 mM $CaCl_2$ and T = 37 °C.

At the oil–water interface (Figure 7), all the assayed BS showed one single maximum located at the same concentration, which appears just slightly higher for NaGDC compared to NaTC and NaGCDC (Figure 7). These maxima of the elasticity (E′) and the concentration range match recent results reported by Wu et al. for NaTC and NaGC adsorbed at the decane–water interface [8]. These authors also suggest that the interfacial complexation of BS through their conjugation groups is responsible for the dilatational response.

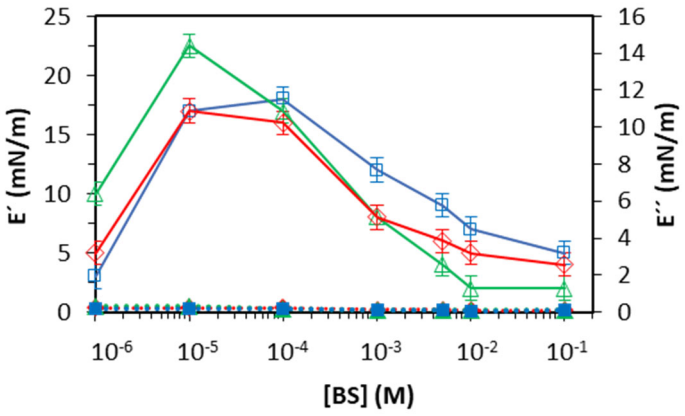

Figure 7. Storage moduli (E′, solid symbols) and loss moduli (E″, open symbols) of NaTC (blue squares), NaGDC (green triangles) and NaGCDC (red rhomboids) at different concentrations of BS ([BS]) at the oil–water interface. Dilatational parameters were measured after 1 h of adsorption at a frequency of 1 Hz in 2 mM Bis-Tris, 150 mM NaCl, 10 mM $CaCl_2$ and T = 37 °C.

In general, BS films display a lower dilatational response at the oil–water interface compared with the air–water interface. Weaker intermolecular interactions in BS films adsorbed at the oil–water interface can originate from the preferred hydrophobic interactions between the molecules of BS and oil, weakening the intermolecular interactions. This effect has also been reported for linear surfactants [21] and proteins [28] at air/oil–water interfaces and suggests that the improved hydrophobic interactions of the oil with molecules of the BS result in a more fluid and mobile interface. However, there are quite a few systems where the hydrophobic interactions of the surfactant with the oil lead to an opposite situation, as reported by Guttman et al. [29], where the hydrophobic interactions of the surfactant with the oil lead to the oil's co-crystallization with the surfactant taking place at an elevated temperature: that is, the interactions lead to a more solid, rather than a more fluid, interfacial layer.

4. Conclusions

The different nature of air/oil–water interfaces clearly affects the rate and degree of adsorption and desorption of surface-active molecules and their surface/interfacial conformation. Results presented here reveal important differences in BS adsorption/desorption at air/oil–water interfaces. A most striking feature is that large differences detected at the air–water interface disappear at the oil–water interface; in this, BS films are rather similar for all BS species. The lack of hydrophobic interactions with the air/solid phase which is present at oil–water interfaces impacts the adsorption/desorption and the dilatational behavior encountered. On one hand, the conjugation groups determine the anchoring at the oil–water interface, while the number/location of hydroxyl groups seems to impact the desorption from the air–water interface. The hydrophobic interactions with conjugates at the oil–water interface determines interfacial complexation, desorption profiles of BS and dilatational moduli. Results presented here advance current knowledge on interfacial mechanisms underlying lipolysis, which, in turn, can have implications on the rational design of food products with tailored digestibility.

Author Contributions: Conceptualization, J.M.-V. and T.d.C.-S.; methodology, T.d.C.-S.; formal analysis, T.d.C.-S.; investigation, T.d.C.-S.; resources, J.M.-V.; data curation, T.d.C.-S.; writing—original draft preparation, T.d.C.-S.; writing—review and editing, J.M.-V.; visualization, T.d.C.-S.; supervision, J.M.-V.; project administration, J.M.-V.; funding acquisition, J.M.-V. All authors have read and agreed to the published version of the manuscript.

Funding: This research was funded by MCIN/AEI/10.13039/501100011033, project PID2020-116615RA-I00. This work was also partially supported by the Biocolloid and Fluid Physics Group (ref. PAI-FQM115) of the University of Granada (Spain). The APC was funded by MDPI and University of Granada.

Institutional Review Board Statement: Not applicable.

Informed Consent Statement: Not applicable.

Data Availability Statement: All data are available in the manuscript.

Conflicts of Interest: The authors declare no conflict of interest.

References

1. Pabois, O.; Ziolek, R.M.; Lorenz, C.D.; Prévost, S.; Mahmoudi, N.; Skoda, M.W.A.; Welbourn, R.J.L.; Valero, M.; Harvey, R.D.; Grundy, M.M.L.; et al. Morphology of Bile Salts Micelles and Mixed Micelles with Lipolysis Products, from Scattering Techniques and Atomistic Simulations. *J. Colloid Interface Sci.* **2021**, *587*, 522–537. [CrossRef]
2. Macierzanka, A.; Torcello-Gómez, A.; Jungnickel, C.; Maldonado-Valderrama, J. Bile Salts in Digestion and Transport of Lipids. *Adv. Colloid Interface Sci.* **2019**, *274*, 102045. [CrossRef] [PubMed]
3. Maldonado-Valderrama, J.; Wilde, P.; MacIerzanka, A.; MacKie, A. The Role of Bile Salts in Digestion. *Adv. Colloid Interface Sci.* **2011**, *165*, 36–46. [CrossRef] [PubMed]
4. Warren, D.B.; Chalmers, D.K.; Hutchison, K.; Dang, W.; Pouton, C.W. Molecular Dynamics Simulations of Spontaneous Bile Salt Aggregation. *Colloids Surf. A Physicochem. Eng. Asp.* **2006**, *280*, 182–193. [CrossRef]
5. Kumar, K.; Chauhan, S. Surface Tension and UV-Visible Investigations of Aggregation and Adsorption Behavior of NaC and NaDC in Water-Amino Acid Mixtures. *Fluid Phase Equilibria* **2015**, *394*, 165–174. [CrossRef]
6. Parker, R.; Rigby, N.M.; Ridout, M.J.; Gunning, A.P.; Wilde, P.J. The Adsorption-Desorption Behaviour and Structure Function Relationships of Bile Salts. *Soft Matter* **2014**, *10*, 6457–6466. [CrossRef] [PubMed]
7. Maldonado-Valderrama, J.; Woodward, N.C.; Patrick Gunning, A.; Ridout, M.J.; Husband, F.A.; Mackie, A.R.; Morris, V.J.; Wilde, P.J. Interfacial Characterization of B-Lactoglobulin Networks: Displacement by Bile Salts. *Langmuir* **2008**, *24*, 6759–6767. [CrossRef] [PubMed]
8. Wu, Y.; Song, R.; Zhao, K.; Bao, Z.; Li, Z.; Zhang, S.; Gao, Y.; Zhang, C.; Du, F. Interfacial Behavior and Emulsion Stability of Lipid Delivery System Regulated by Two-Dimensional Facial Amphiphiles Bile Salts. *J. Mol. Liquids* **2022**, *362*, 119744. [CrossRef]
9. Maldonado-Valderrama, J.; Muros-Cobos, J.L.; Holgado-Terriza, J.A.; Cabrerizo-Vílchez, M.Á. Bile Salts at the Air-Water Interface: Adsorption and Desorption. *Colloids Surf. B Biointerfaces* **2014**, *120*, 176–183. [CrossRef]
10. Łozińska, N.; Jungnickel, C. Importance of Conjugation of the Bile Salt on the Mechanism of Lipolysis. *Molecules* **2021**, *26*, 5764. [CrossRef]

11. Pérez-Mosqueda, L.M.; Maldonado-Valderrama, J.; Ramírez, P.; Cabrerizo-Vílchez, M.A.; Muñoz, J. Interfacial Characterization of Pluronic PE9400 at Biocompatible (Air-Water and Limonene-Water) Interfaces. *Colloids Surf. B Biointerfaces* **2013**, *111*, 171–178. [CrossRef] [PubMed]
12. Maldonado-Valderrama, J.; Fainerman, V.B.; Gálvez-Ruiz, M.J.; Martín-Rodriguez, A.; Cabrerizo-Vílchez, M.A.; Miller, R. Dilatational Rheology of β-Casein Adsorbed Layers at Liquid−Fluid Interfaces. *J. Phys. Chem. B* **2005**, *109*, 17608–17616. [CrossRef] [PubMed]
13. Maldonado-Valderrama, J.; Martin-Molina, A.; Galvez-Ruiz, M.J.; Martin-Rodriguez, A.; Cabrerizo-Vilchez, M.A. Beta-Casein Adsorption at Liquid Interfaces: Theory and Experiment. *J. Phys. Chem. B* **2004**, *108*, 12940–12945. [CrossRef]
14. Brodkorb, A.; Egger, L.; Alminger, M.; Alvito, P.; Assunção, R.; Ballance, S.; Bohn, T.; Bourlieu-Lacanal, C.; Boutrou, R.; Carrière, F.; et al. INFOGEST Static in Vitro Simulation of Gastrointestinal Food Digestion. *Nat. Protoc.* **2019**, *14*, 991–1014. [CrossRef] [PubMed]
15. Maldonado-Valderrama, J.; Holgado-Terriza, J.A.; Torcello-Gómez, A.; Cabrerizo-Vílchez, M.A. In Vitro Digestion of Interfacial Protein Structures. *Soft Matter* **2013**, *9*, 1043–1053. [CrossRef]
16. del Castillo-Santaella, T.; Sanmartin, E.; Cabrerizo-Vílchez, M.Á.; Arboleya, J.C.; Maldonado-Valderrama, J. Improved Digestibility of b -Lactoglobulin by Pulsed Light Processing: A Dilatational and Shear Study. *Soft Matter* **2014**, *10*, 9702–9714. [CrossRef]
17. Cabrerizo-Vílchez, M.A. Coaxial Capillary and Exchange Procedure for Penetration Surface Scale. Spanish Patent P9801626, 1 September 2001.
18. Maldonado-Valderrama, J.; del Castillo-Santaella, T.; Holgado-Terriza, J.A.; Cabrerizo-Vílchez, M.Á. In Vitro Digestion of Emulsions in a Single Droplet via Multi Subphase Exchange of Simulated Gastrointestinal Fluids. *J. Vis. Exp.* **2022**, *189*, e64158. [CrossRef]
19. Maldonado-Valderrama, J.; Torcello-Gómez, A.; Del Castillo-Santaella, T.; Holgado-Terriza, J.A.; Cabrerizo-Vílchez, M.A. Subphase Exchange Experiments with the Pendant Drop Technique. *Adv. Colloid Interface Sci.* **2015**, *222*, 488–501. [CrossRef]
20. Ravera, F.; Loglio, G.; Kovalchuk, V.I. Interfacial Dilational Rheology by Oscillating Bubble/Drop Methods. *Curr. Opin. Colloid Interface Sci.* **2010**, *15*, 217–228. [CrossRef]
21. Bergfreund, J.; Siegenthaler, S.; Lutz-Bueno, V.; Bertsch, P.; Fischer, P. Surfactant Adsorption to Different Fluid Interfaces. *Langmuir* **2021**, *37*, 6722–6727. [CrossRef]
22. O'Connor, C.J.; Ch'ng, B.T.; Wallace, R.G. Studies in Bile Salt Solutions: 1. Surface Tension Evidence for a Stepwise Aggregation Model. *J. Colloid Interface Sci.* **1983**, *95*, 410–419. [CrossRef]
23. Wojciechowski, K. Surface Activity of Saponin from Quillaja Bark at the Air/Water and Oil/Water Interfaces. *Colloids Surf. B Biointerfaces* **2013**, *108*, 95–102. [CrossRef] [PubMed]
24. Poirier, A.; Stocco, A.; Kapel, R.; In, M.; Ramos, L.; Banc, A. Sunflower Proteins at Air-Water and Oil-Water Interfaces. *Langmuir* **2021**, *37*, 2714–2727. [CrossRef]
25. Lentzi, P.; Georgiou, D.; Kalogianni, E.P.; Kyriakoudi, A.; Ritzoulis, C. Emulsifiers from White Beans: Extraction and Characterization. *Colloids Interfaces* **2022**, *6*, 71. [CrossRef]
26. Dowlati, S.; Javadi, A.; Miller, R.; Eckert, K.; Kraume, M. Unfolded Lipase at Interfaces Studied via Interfacial Dilational Rheology: The Impact of Urea. *Colloids Interfaces* **2022**, *6*, 56. [CrossRef]
27. Langevin, D. Influence of Interfacial Rheology on Foam and Emulsion Properties. *Adv. Colloid Interface Sci.* **2000**, *88*, 209–222. [CrossRef]
28. Kontogiorgos, V.; Prakash, S. Adsorption Kinetics and Dilatational Rheology of Plant Protein Concentrates at the Air- and Oil-Water Interfaces. *Food Hydrocoll.* **2023**, *138*, 108486. [CrossRef]
29. Guttman, S.; Ocko, B.M.; Deutsch, M.; Sloutskin, E. From Faceted Vesicles to Liquid Icoshedra: Where Topology and Crystallography Meet. *Curr. Opin. Colloid Interface Sci.* **2016**, *22*, 35–40. [CrossRef]